ACCEPTED MANUSCRIPT • OPEN ACCESS

Large-range high-speed dynamic-mode atomic force microscope imaging: adaptive tapping towards minimal force

To cite this article before publication: Jiarong Chen et al 2023 Nanotechnology in press https://doi.org/10.1088/1361-6528/acd700

Manuscript version: Accepted Manuscript

Accepted Manuscript is "the version of the article accepted for publication including all changes made as a result of the peer review process, and which may also include the addition to the article by IOP Publishing of a header, an article ID, a cover sheet and/or an 'Accepted Manuscript' watermark, but excluding any other editing, typesetting or other changes made by IOP Publishing and/or its licensors"

This Accepted Manuscript is © 2023 The Author(s). Published by IOP Publishing Ltd.

As the Version of Record of this article is going to be / has been published on a gold open access basis under a CC BY 4.0 licence, this Accepted Manuscript is available for reuse under a CC BY 4.0 licence immediately.

Everyone is permitted to use all or part of the original content in this article, provided that they adhere to all the terms of the licence https://creativecommons.org/licences/by/4.0

Although reasonable endeavours have been taken to obtain all necessary permissions from third parties to include their copyrighted content within this article, their full citation and copyright line may not be present in this Accepted Manuscript version. Before using any content from this article, please refer to the Version of Record on IOPscience once published for full citation and copyright details, as permissions may be required. All third party content is fully copyright protected and is not published on a gold open access basis under a CC BY licence, unless that is specifically stated in the figure caption in the Version of Record.

View the article online for updates and enhancements.

Large-range High-speed Dynamic-mode Atomic Force Microscope Imaging: Adaptive Tapping towards Minimal Force

Jiarong Chen¹ and Qingze Zou²

Department of Mechanical and Aerospace Engineering, Rutgers University, Piscataway, NJ 08854, USA

E-mail: jiarong.chen@rutgers.edu and qzzou@rci.rutgers.edu

November 2022

Abstract. In this paper, a software-hardware integrated approach is proposed for high-speed large-range dynamic mode imaging of atomic force microscope (AFM). High speed AFM imaging is needed in various applications, particularly in interrogating dynamic processes at nanoscale such as polymer crystallization process. Achieving high speed in tapping-mode AFM imaging is challenging as the probe-sample interaction during the imaging process is highly nonlinear, making the tapping motion highly sensitive to the probe sample spacing, and thereby, difficult to maintain at highspeed. Increasing the speed via hardware bandwidth enlargement, however, leads to a substantially reduction of imaging area that can be covered. Contrarily, the imaging speed can be increased without loss of the scan size through control (algorithm)-based approach, for example, the recently developed adaptive multiloop mode (AMLM) technique, has demonstrated its efficacy in increasing the tapping-mode imaging speed without loss of scan size. Further improvement, however, has been limited by the hardware bandwidth and online signal processing speed and computation complexity. Thus, in this paper, the AMLM technique is further enhanced to optimize the probe tapping regulation and integrated with a field programmable gate array (FPGA) platform to further increase the imaging speed without loss of quality and scan range. Experimental implementation of the proposed approach demonstrates that the high-quality imaging can be achieved at a high-speed scanning rate of 100 Hz and higher, and over a large imaging area of over 20 μ m.

1. INTRODUCTION

In this paper, we present a large-range dynamic-mode atomic force microscope (AFM) imaging, with the scanning speeds significantly faster (4 to 5 times faster) than those reported in the literature, achieved through the development of a control-based imaging technique with adaptive tapping towards minimal normal force. Dynamic-mode, particularly, tapping mode (TM) [1] and its extensions such as peakforce QNM [12, 13], has become the *de facto* choice of AFM imaging technique for its high quality imaging

quality and subdued sample distortion. The imaging speed of tapping mode, however, is significantly slower than that of contact mode (CM) imaging [1]. It is much more challenging, due to the highly nonlinear probe sample contact [3], to maintain a stable probe-sample contact in tapping mode imaging, especially when the scan size becomes large [4]. Although existing efforts have been made to increase the speed of tapping mode imaging through hardware and software (algorithm) innovations [5–7], these efforts are limited in the imaging speed that can be achieved—without loss of imaging quality, or the sample size that can be scanned (per image). Thus, this work is motivated to substantially increase the tapping mode imaging speed at large scan size.

High-speed tapping mode imaging over a large scan size without loss of imaging quality faces challenges to overcome. Inherently, the imaging speed is limited by the highly nonlinear force-distance relation during the tapping of the probe on the sample surface when the probe scans across the sample surface [8]. As a result, the tapping amplitude is sensitive to the variation of the probe-sample distance. Thus, when the sample topography varies dramatically, the tapping amplitude can quickly change significantly [9]. This sudden change of the tapping amplitude, as the probe scans across the sample at high speed, can lead to a loss of probe contact, or annihilation of the tapping motion [2, 9]. As the tapping amplitude must be closely regulated, the loss of contact and/or tapping annihilation directly results in imaging quality degradation, and sample and/or probe deformation [4,9]. Maintaining the tapping amplitude during high-speed imaging is further complicated by the time-delay [10] in deciphering the tapping amplitude as the tip is vibrating around he resonance of the cantilever [17]. Thus, maintaining the probesample distance upon sample topography variation is essential to high-speed tapping mode imaging.

Limitations exist in current efforts to achieve high-speed, tapping mode imaging at large scan range. For example, the tapping mode imaging speed can be increased through hardware improvements [10, 14, 15] by substantially increasing the bandwidth of the overall nanopositioning system along with high-speed data processing. The idea is that as such, the scanning rate can be increased accordingly while still stays well below the bandwidth, and the dynamics of the AFM system is not excited. This increase of scanning rate, however, is accompanied with a dramatic reduction of imaging area—the sample area covered per image is reduced by over 2 orders of magnitude (e.g., from $100 \times 100 \ \mu m^2$ to around $2 \times 2 \ \mu m^2$ and less) [7], due to the inherent physical limitation that actuator displacement range reduces as its bandwidth increases [15]. To increase the imaging speed—without losing the scan size, more advanced control techniques than the conventional PID control have been developed [20–22]. For example, the time-delay in deciphering the tapping amplitude can be reduced, and thereby, the sample topography can be better estimated by observer-based techniques [16, 19, 25]. Recent efforts in improving the performance or functionality of tapping-mode or peak-force mode imaging also include the double-pass scanning method [11] to compensate for cantilever deflec-

Large-range High-speed Dynamic-mode Atomic Force Microscope Imaging

tion drift and environmental disturbance (e.g., hydrodynamic force in liquid imaging), and the PeakForce Quantitative Nanomechanics (PF-QNM) technique [12,13] that combines peak force imaging with infrared reflection mapping to simultaneously map sample topography and chemical-mechanical properties of the sample. These techniques, however, are not focused on increasing the speed of TM imaging, and the challenges above in high-speed imaging still exist.

These limitations of control technique developments in improving tapping mode imaging have been tackled in the recent-developed adaptive multi-loop mode (AMLM) [2,24] technique. The main idea is to introduce an additional feedback loop to regulate the mean value of the probe vibration (called the TM-deflection), and thereby, regulate the interaction force, and then, augment a data-driven online iterative feedforward control to enhance the tracking of the sample topography. Experimental results obtained on various polymer samples showed that over an order of magnitude increase of the imaging speed can be achieved in large-range imaging without loss of imaging quality (over 50 μ m) [2]—at scanning rate at 20-25 Hz. Further increase of the imaging speed, however, has been limited by the hardware bandwidth, the online signal processing speed and the computation complexity (in the frequency-domain iterative control algorithm involved). Therefore, we propose to address these limitations to further improve the technique.

We develop a hardware-software-integrated approach towards high-speed large-range tapping mode imaging. First, to optimize the tapping amplitude regulation, we propose to online regulate via a local feedback control, the setpoint of the tapping amplitude adaptively around the optimal value. In contrast, in all existing tapping mode techniques the setpoint of the tapping amplitude is set at a pre-chosen constant. Then, a data-driven, time-domain, inversion-based iterative control is proposed to replace the frequency-domain one in the AMLM technique. As such, the complicated online computation in frequency-domain are eliminated. Moreover, To further improve the sample topography tracking, the estimation of the sample topography on the previous scan line (used as the desired trajectory to be tracked on the current scan line) is improved by taking into account of the tracking errors in both the tapping amplitude and the TM-deflection regulation. This enhanced AMLM technique is implemented on a field programmable gate array (FPGA)-based platform with high-speed online signal acquisition and processing. Methods to circumvent the hardware limitations of current FPGA system (e.g., limited onboard memory) are also discussed. This FPGA-based enhanced AMLM technique is applied to an AFM with higher bandwidth piezoelectric actuation system (nearly 10 times larger than that previously). Such an integrated approach merges, in a synergistic manner, the advantages of both hardware and software together for high-speed tapping mode imaging at large scan size. Experimental implementation results are presented to show that tapping mode imaging at large-range (scan size at over 21 μ m) and high-speed (with scanning rate at 100 to 120 Hz) can be achieved on samples of high aspect ratio, while maintaining the imaging quality. Preliminary

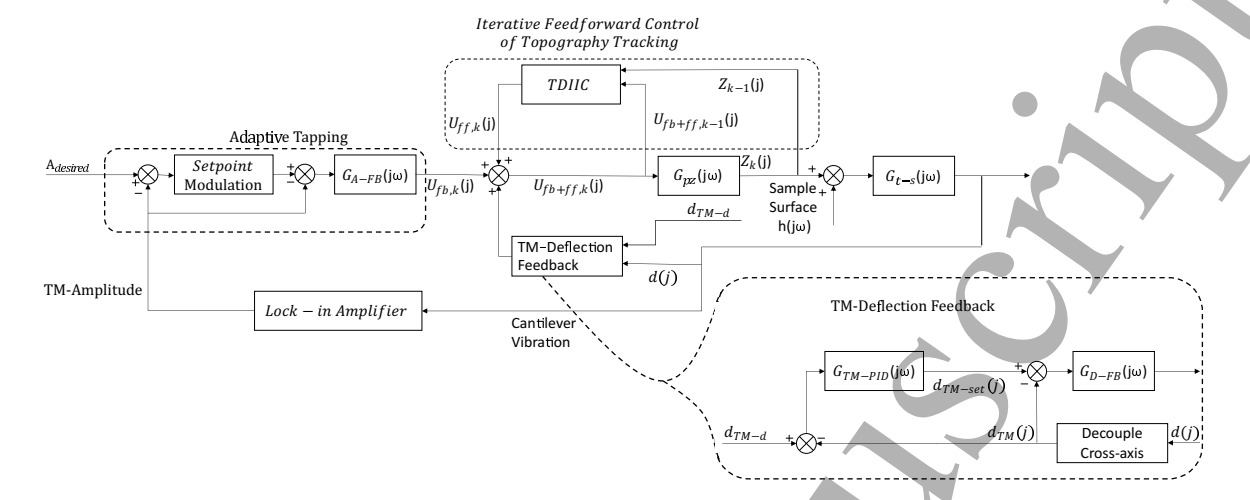


Figure 1. Schematic block diagram of the AT-MLM imaging

results of this work has been reported in a recent conference [18]. Here we substantially expanded and extended the work with adaptive tapping modulation to minimize the tapping force, doubled the imaging speed, and enlarged the scanning area size.

2. High-Speed Large-Range Dynamic-mode Imaging: An Integrated Approach

We propose to address the challenges in high-speed tapping mode imaging at large scan size. During tapping mode imaging, the cantilever probe is excited by a dither piezo to vibrate near its resonance frequency and tap on the surface constantly [26]. Then the amplitude of the probe tapping is measured (e.g., through a lock-in amplifier) and regulated around the pre-chosen set-point value while the probe is scanning across the sample surface, and the sample topography can be quantified as the vertical displacement of the piezoelectrical actuator—provided that the tapping amplitude is closely regulated. However, the speed of conventional tapping mode imaging is inherently hampered by the slow response of the tapping amplitude regulation feedback, and the tapping being sensitive to the probe-sample distance due to the highly nonlinearity of the probe-sample interaction force [9]. As the imaging speed increases, loss of probe-sample contact tends to occur when the topography suddenly drops, and the tapping can be completely annihilated around regions where the sample topography rises dramatically. [18]

The adaptive tapping multi-loop mode (AT-MLM), as depicted in Fig. 1, is proposed by extending the AMLM technique [2] to adaptively tune the tapping amplitude (TA) online towards the minimization of the tapping force (the "Adaptive Tapping" part in Fig. 1). Moreover, the iterative feedforward control of the sample topography tracking in the AMLM method is further enhanced by accounting for both the tapping amplitude and the mean value of the probe tapping vibration (called the *TM-deflection*

below), and simplifying the online iterative control with a time-domain data-driven algorithm (the "Iterative feedforward control of topography tracking" part in Fig 1). As in the AMLM technique, a feedback control of inner-outer loop structure is integrated to regulate the TM-deflection (the "TM-Deflection Feedback" part in Fig. 1). We start with introducing the adaptive tapping first.

2.1. Adaptive Tapping towards Force Minimization

In contrast to other existing dynamic mode imaging methods where the TA-set point is pre-chosen and fixed, in the proposed AT-MLM approach the set-point of the tapping amplitude is adjusted and tuned online during the scanning process. As such, it opens the door to optimize the cantilever tapping, e.g., minimizing the tapping force. The TA-set point is adjusted to ensure that loss of probe-sample contact or annihilation of tapping is avoided during the imaging process, making it more flexible, and thereby, potentially easier to track the sample topography, particularly when the scanning speed increases. Thus, this idea extends the adaptive adjustment of the deflection setpoint in contact mode imaging to minimize the normal force [3]. The TA-setpoint is adjusted through a gradient descend online adjustment:

$$A_{set}(j+1) = \begin{cases} A_{set}(j) + \rho[A_{opt} - A_{set}(j))], & \text{if } |e_k(j) - e_k(j-1)| < \delta \\ A_p, & \text{otherwise} \end{cases}$$
where $e_k(j) = A(j) - A_{set}(j)$ (2)

where
$$e_k(j) = A(j) - A_{set}(j)$$
 (2)

where $j = 2, ..., \mathcal{N}_s - 1$, with \mathcal{N}_s the total number of sampling points per scan line, A_{opt} is the TA-setpoint corresponding to the minimal probe-sample interaction force, A_p is the setpoint that ensures a stable probe tapping and maintains the image quality, ρ is the step size, and δ is the pre-chosen threshold, respectively.

Thus in the above adaptive tapping, the TA-set-point is online adjusted towards the minimal tapping force when the fluctuation of the TA-error $e_k(j)$ is small (within the threshold value δ). Other methods to adaptively adjust the tapping amplitude might be utilized, for example, based on optimal control. The outer-inner feedback control structure is proposed here for its ease of implementation, e.g., the existing tapping-amplitude feedback control is intacted.

When the normalized TA (with respect to the probe vibration amplitude without tapping on the sample surface) is smaller than 10%, the tip-sample interaction force increases significantly, while the probe-sample contact can be easily lost as scanning speed increases when the normalized TA is larger than 80% [8]. Therefore, the normalized TA A_{set} shall be maintained within the range of 10% to 30% to ensure the image quality and keep the interaction force small. If the tapping amplitude is well maintained in this range, the setpoint can be increased to reduce the tapping force, or

the setpoint is reset to ensure the imaging quality. The change of the TA-setpoint needs to be accounted in the sample topography quantification (discussed later in Sec. III.C).

2.2. TM-Deflection Regulation via Inner-outer Feedback Control

As in the AMLM approach [2], a feedback loop is introduced to regulate the TM-deflection. Working together with the above TA feedback loop in concert, this TM-deflection feedback loop is to optimize and maintain a stable probe tapping during the imaging. Similar to the above TA-loop, the TM-deflection is regulated through an inner-outer feedback loop, where the outer loop is to adjust the TM-deflection setpoint through the following PID type of control (see Fig. 2) [18],

$$d_{TM_set}(j+1) = k_{p,m}e_{TM}(j) + k_{i,m}d_{TM_set}(j) + k_{d,m}[e_{TM}(j-1) - e_{TM}(j)](3)$$

$$e_{TM}(j) = d_{TM_d} - d_{TM}(j) \tag{4}$$

and $j = 2, ..., \mathcal{N}_s - 1$, where \mathcal{N}_s is the total number of sampling periods per scan line, and $k_{p,m}$, $k_{i,m}$, and $k_{d,m}$ are the proportional, integral, and derivative coefficients, respectively. Initially the setpoint for the outer loop d_{TM_d} is set as the mean TM deflection at the starting point of the imaging process.

Compensation for the Lateral-to-vertical Coupling

To integrate the above TM-deflection loop to state-of-the-art AFM systems using small-size cantilevers (e.g., the FASTSCAN system, Bruker Nano. Inc.), the deviation caused by the lateral-to-vertical coupling to the TM-deflection must be accounted for. The amplitude of the variation can be ten times larger than that caused by the sample to-pography variation.

An experiment-based decoupling method is employed to remove this lateral-to-vertical coupling effect. First, the coupling-caused TM-deflection is obtained by acquiring the signal through a so-called *pseudo-imaging* process during which the cantilever scans, without touching the surface, over the same imaging area at the same scanning speed as in the targeted imaging process. Then, during the targeted imaging process later, the acquired TM deflection signal will be subtracted from the measured one, and used in both the above TM-deflection feedback loop and the feedforward control, as well as in the topography construction, i.e.,

$$d_{TM}(j) = d(j) - d_p(j) \tag{5}$$

where $d_{TM}(j)$ is the coupling-free TM deflection, d(j) is the raw deflection and $d_p(j)$ is the TM deflection acquired by the pseudo-imaging process. Compared to other model-based methods, this procedure is more effective as the coupling can vary substantially in different cantilever condition but remains largely the same for the imaging process followed—the cantilever used and its mount and the environment condition are the same.

2.3. Time-domain Online iterative feedforward control for sample-topography tracking

Sample Topography Quantification First, the sample topography tracked in the feedforward control is quantified. The change of TA-set point and the errors in tracking the TA and the TM-deflection are accounted for in the quantification of the sample topography: The sample topography of k^{th} scan line $h_{k,t}(j)$ is quantified as

$$h_{k,t}(j) = h_{k,z}(j) + k_{h,a}e_{k,Amp}(j) + k_{h,m}e_{k,TM}(j), \text{ for } j = 0, 1, 2, ..., N - 1(6)$$

where $h_{k,z}(j)$ is the z-axis piezo displacement of k^{th} scan line, $k_{h,a}$ and $k_{h,m}$ are the corresponding scale factors from tapping amplitude error and deflection error to piezo displacement, $e_{k,Amp}(j)$ and $e_{k,TM}(j)$ are the tapping amplitude error and deflection error of k^{th} scan line, respectively acquired during imaging process.

Time-domain Inversion-based Iterative Control (TDHC) Then, a data-driven iterative feedforward control is employed to track the sample topography, similar to the AMLM technique [2]. To enhance the online implementation efficacy—critical to the targeted high speed imaging in this work (e.g., at scanning rate of 120 Hz), the frequency-domain IIC algorithm in the AMLM method [2] is replaced with the following time-domain inversion-based iterative control (TDIIC) algorithm,

$$u_{ff,0}(j) = 0,$$
 (7)

$$u_{ff,0}(j) = 0,$$
 (7)
 $u_{ff,k+1}(j) = k_{inv}(j)h_{k+1,d}(j) = k_{inv}(j)h_{k,t}(j)$ for $j = 0, 1, 2, ..., N - 1$ (8)

where, respectively, $k_{inv}(j)$ is the iterative gain updated point-by-point, and $h_{k+1,d}(\cdot)$ is the desired sample topography to track in the $k+1^{th}$ iteration, estimated by using the k^{th} estimation, $h_{k,t}(\cdot)$ (see Eq.6). Moreover, the iterative gain $k_{inv}(j)$ is updated by using the measured input-output data as

$$k_{inv}(j) = \begin{cases} (1 - \lambda)k_{inv,DC} + \lambda \frac{u_{ff+fb,k}(j)}{h_k(j)} & \text{if } |\delta h(j)| \le \epsilon \\ k_{inv,DC} & \text{otherwise} \end{cases}$$
(9)

where $k_{inv,DC}$ is the inverse DC-gain of the z-axis AFM piezo-actuation system, and $\delta h(j)$ is the velocity of the probe given by

$$\delta h(j) = h_{k-1,d}(j) - h_{k-1,d}(j-1) \tag{10}$$

The online adjustment of the iterative gain $k_{inv}(\cdot)$ is to account for the variation of the system gain with the saturation effect considered. The threshold value ϵ is chosen based on the probe velocity, as the variation of the gain k_{inv} grows with the probe velocity due to its nonlinear dynamics [18].

At the beginning of the imaging process, the scheme described above is applied to scan on the first line repetitively until convergence is reached, (i.e., the difference of the z-piezo displacement between two consecutive iterations converges towards the noise level of the signal). Then the rest of the sample is scanned continuously without

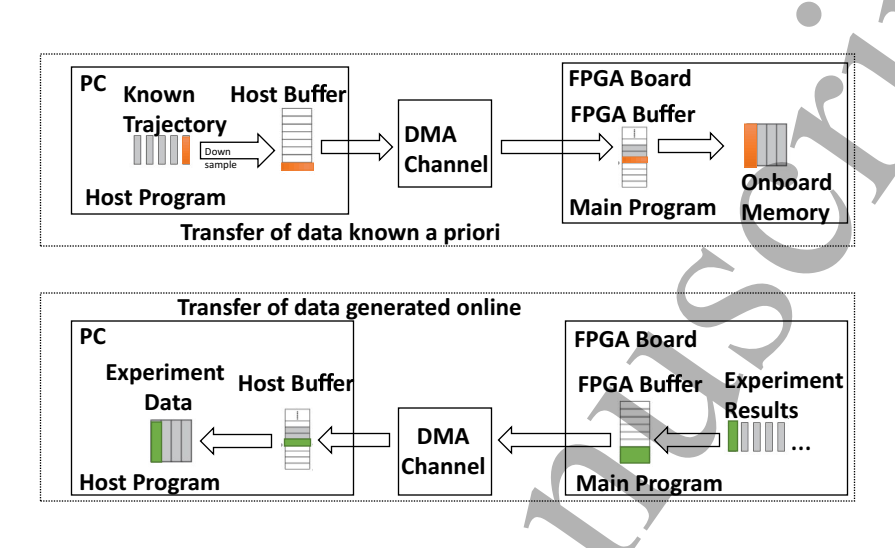


Figure 2. Schematic block diagram of the method for FPGA transferring (a) large-size data known a priori, and (b) those generated/modified online, respectively.

repetition [18].

A summary of the proposed method is presented as Algorithm 1 in next page.

3. FPGA-based Online Implementation

A FPGA-based signal processing platform is utilized to materialize the proposed approach, providing the needed sampling rate and online computation capability for high-speed AFM imaging.

To implement control algorithms involving both feedforward and feedback loops for trajectory tracking (such as the tracking of the sample profile in the proposed approach), issues caused by limited onboard memory must be addressed, as the desired trajectory to track or the image data acquired online cannot be entirely stored onboard during the experiment process. For large-size data known a priori (e.g., a desired trajectory), the data are downsampled on the host computer before the transfer and then online recovered on the FPGA board via interpolation (See Fig. 2(a)) [18]. Contrarily, data generated or modified online, are transferred to the host computer simultaneously during the experiment process through a buffer-to-buffer structure implemented via the direct-memory-access (DMA) technique, without interfering with online operations (e.g., sampling and computation) (see Fig. 2(b)). Additional care shall also be taken to

```
Large-range High-speed Dynamic-mode Atomic Force Microscope Imaging
```

```
Algorithm 1: Adaptive Tapping Multi-loop Mode (AT-MLM)
   Input: Measured tapping amplitude A(j), tapping deflection d(j), z-axis
              sensor signal h_{k,z}(j), number of scan lines N_{\ell}, and number of
              samples each line N_s, parameters \delta, \lambda, and \epsilon
   Output: Control output u_k(j)
 1 for k = 1; k < N_{\ell}; k = k + 1 do
       for j = 0; j < N_s - 1; j = j + 1 do
 \mathbf{2}
           /* Adaptive tapping amplitude setpoint modulation
           Compute the tapping amlitude error e_{k,Amp}(j) = A(j) - A_{set}(j)
 3
           if |e_{k,Amp}(j+1) - e_{k,Amp}(j)| < \delta then
 4
            A_{set}(j+1) = A_{set}(j) + \rho[A_{opt} - A_{set}(j)]
 5
           end
 6
           else
 7
            A_{set}(j+1) = A_p
 8
           end
 9
           Use A_{set}(j) as the setpoint to PID controller G_{A-FB}(j\omega) to generate
10
            output u_{fb-a,k}(j)
           /* Tapping mode-deflection regulation via inner-outer
               feedback
           d_{TM}(j) = d(j) - d_{p}(j)
                                                   // Lateral-to-vertical coupling
11
            compensation
           e_{k,TM}(j) = d_{TM-d} - d_{TM}(j);
                                                        // Tapping deflection error
12
           d_{TM\_set}(j+1) =
13
            k_{p,m}e_{k,TM}(j) + k_{i,m}d_{k,TM\_set}(j) + k_{d,m}[e_{k,TM}(j-1) - e_{k,TM}(j)]
           Use d_{TM-set}(j) as the setpoint to PID controller G_{D-FB}(j\omega) to
14
            generate output u_{fb-d,k}(j)
           /* Time-domain online iterative feedforward control
                                                                                          */
           if k=0 then
15
               u_{ff,k}(j) = 0
16
           \operatorname{end}
17
           else
18
               if |h_{k-1,t}(j+1) - h_{k-1,t}(j)| < \epsilon then
19
                  k_{inv}(j) = (1 - \lambda)k_{inv,DC} + \lambda \frac{U_{ff+fb,k-1}(j)}{h_{k-1}(j)}
20
               end
21
               else
22
                   k_{inv}(j) = k_{inv.DC}
23
               end
24
25
           h_{k,t}(j) = h_{k,z}(j) + k_{h,a}e_{k,Amp}(j) + k_{h,m}e_{k,TM}(j)
26
           u_k(j) = u_{fb-a,k}(j) + u_{fb-d,k}(j) + u_{ff,k}(j)
27
       end
28
29 end
```

Large-range High-speed Dynamic-mode Atomic Force Microscope Imaging

allocate and assign buffers along with the DMA channels to avoid data overlap or lost, as there are only few DMA channels onboard and that are half-duplex, too. In implementation, the proposed technique is implemented as a project on the FPGA platform along with a computer (see Fig. 2). The project consists a "host program", run on the host computer, and a "main program" that was complied into the FPGA bit-code, and ran on the FPGA card. The "host program" controls the data transfer between the host computer and the FPGA card (see Fig. 2), and the proposed technique is implemented in the "main program", respectively.

4. Experimental Example

The proposed technique was implemented in an AFM imaging experiments. The objective is to demonstrate that by using the proposed technique, high-quality, high-speed imaging can be achieved over a large scan size. We start with describing the experimental setup.

Experimental Setup

The experiments were performed on a state-of-the-art AFM system (Dimension FastScan, Bruker Inc), where, for implementing external control of AFM operation, the internal built-in control of the AFM can be bypassed, the piezoelectrical actuators can be directly controlled through external inputs, and the cantilever displacements in x-, y- and z-axes and the probe-sample interaction force (the cantilever deflection) can be directly measured (through a signal module box of the AFM system. Similar direct sensor access was applied in other commercial SPM systems). The bypass of the internal control and the direct sensor and drive signal accesses was provided by the AFM manufacturer (most AFM companies can provide such minor hardware modification at a small to no cost). A FPGA-based DAQ system (NI RIO Device, USB-7856R, National Instrument Inc.) was used along with a host PC (Asus G14 GA401 laptop with AMD Ryzen 7 4800HS CPU and 16 Gb RAM) to implement the proposed AT-MLM technique, and the data obtained were processed using Matlab-Simulink (Mathworks Inc.). The sampling rate was set at 200 kHz, and a calibration sample (STR3-1800P, Bruker Inc. with 180nm step height and $1.5\mu m$ pitches separated by $1.5 \mu m$ spacing) was imaged with a lateral scanning size at 21 μ m. The displacement deviation caused by hysteresis at such a scan range was more than 22%. A blend of Polystyrene and Polyolefin Elastomer (PS-LDPE) sample was also imaged to further assess the proposed technique.

Experimental Implementation

First, the lateral-coupling effect was accounted for by using the proposed pseudo-imaging technique (see Sec. III.B). The TM-deflection signal was acquired without sample-probe

Large-range High-speed Dynamic-mode Atomic Force Microscope Imaging

11

contact, and the lateral scanning size was kept the same as those used in later imaging experiment. The scanning speed was set at 50 Hz and the TM-deflection signal acquired through the pseudo-imaging process was used as the baseline TM-deflection signal $d_n(j)$ (in Eq. (5)) to be subtracted to remove the lateral-coupling from the measured TM deflection in all the experiments at three different scanning speeds (50 Hz, 100 Hz and 120 Hz). Then, the proposed AT-MLM technique was applied. First, the PID parameters of the TM-amplitude loop and the cut-off frequency of the low pass filter were adjusted under the conventional tapping mode (i.e., with only the TM-amplitude feedback and a constant TM-amplitude set-point value), through the step response of the TM-amplitude closed-loop system, under a stable tapping on a hard sample (e.g., the calibration sample above) without lateral scanning. The experimentally-tuned optimal settling time and the optimal overshoot obtained were 0.56 milliseconds with 12% overshoot, respectively, and the desired topography $h_{k,d}(j)$ was filtered by low pass filter whose cut-off frequency was chosen at 3000 Hz based on the estimated spectrum of the topography signal at the scan rate of 100 Hz. Then, the coefficients of both the TM-amplitude and the TM-deflection loop were tuned experimentally, respectively, by following the same procedure and the similar criteria. Once these three loops worked together properly, the TDIIC feedforward control was augmented (see Eq. (6)), where the scaling factors of the TM-amplitude error and the TM-deflection error, respectively, were adjusted by using the calibration sample above.

During the implementation of the AT-MLM method, the sample was first scanned by using the TM-ampltitude feedback alone at low scan rate of 2 Hz on the first scan line, i.e., without augmenting the iterative feedforward control and the TM-deflection loop, to obtain an accurate tracking of the sample topography profile of the first scan line. Then the time-domain iterative feedforward control was augmented, along with the TM-deflection feedback loop and the adaptive tapping mode amplitude regulation loop, where the sample topography obtained via at 2 Hz was used as the initial desired trajectory. The sample was then imaged at the chosen high-speed scan rate repetitively on the first line for four times (see Fig. 5) to ensure the convergence and thereby, accurate in tracking of the sample topography. Next, the rest of the sample area was imaged without repetitive scanning, with the desired trajectory for the TDIIC feedforward constructed by using the signals acquired in the previous scanline (see Eq.(6)). Precision scanning in the lateral x- and y- axes were obtained by using the MIIC technique [27], where the lateral scanning tracking error was maintained below 1.2 % (measured in the relative 2-norm sense), respectively. For comparison, images of both the calibration sample and the PS-LDPE sample were also obtained by using the conventional TMimaging at the three scanning rates of 50 Hz, 100 Hz, and 120 Hz, respectively.



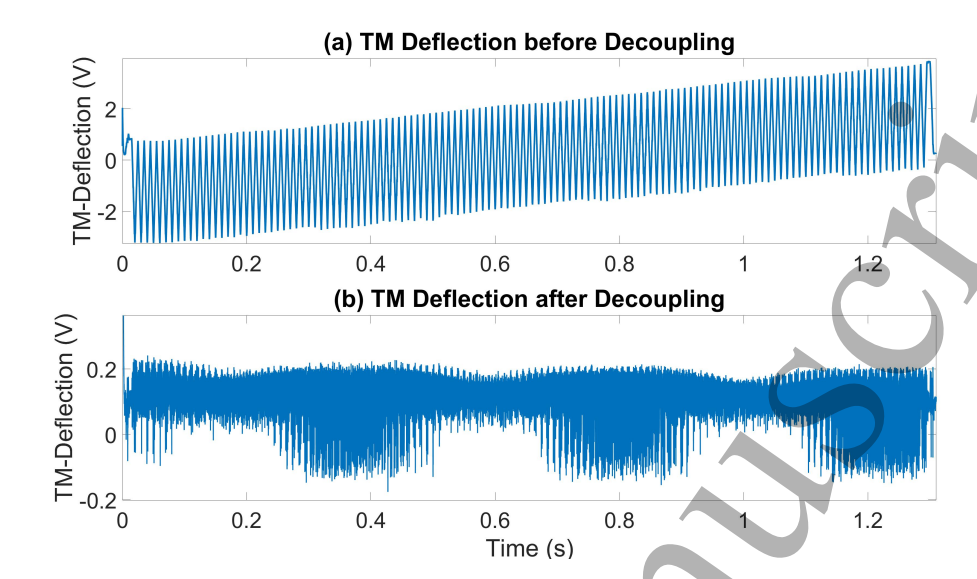


Figure 3. Comparison of (a) the measured TM-deflection under lateral coupling effect (scan rate: 100 Hz), and (b) that after the coupling compensation, respectively.

Experimental Results and Discussion

The experimental results obtained are presented in Figs. 3 to 10. The lateral-couplingcaused TM-deflection variation measured at the scan rate of 50 Hz is shown in Fig. 3 (a), compared to that after the coupling removal in Fig. 3 (b), respectively. To examine the convergence of the TD-IIC in the proposed AT-MLM approach, the z-axis tracking results obtained in the four online repetitive scannings on the first scan line (scan rate: 100 Hz) are shown in Fig. 4, compared to that obtained by using the PI-feedback control at low speed (scan rate of 2 Hz). The relative 2-norm of the tracking error with respect to the 2-Hz PI-tracking in each iteration, $\mathbf{E}_{k,2}(\%)$, is shown in Fig. 5. To assess the effectiveness of the adaptive adjustment of the TM-amplitude set-point, $A_{set}(j)$, the online adjusted $A_{set}(j)$ and the tapping amplitude ratio $A(j)/A_{free}$ (A_{free} is the free tapping amplitude) are shown in Fig. 6. The topography images obtained by using the proposed AT-MLM technique at the scan rate of 100 Hz is compared to that by using the PI-control at the scan rate of 2 Hz and 100 Hz in Fig. 7, respectively, where the image obtained by using the adaptive tapping technique and TD-IIC feedforward control (Fig. 7 (c)) is also shown to evaluate the effectiveness of the proposed adaptive adjustment of TM-amplitude set-point. To further validate the proposed approach, the topography images obtained at other two scan rates (50 Hz and 120 Hz) are compared to the PI-control results in Fig. 8, and the images of the LDPE sample obtained by these two methods are also compared in Fig. 9 for all the three scan rates, respectively. The relative 2-norm errors over the entire image for the proposed technique are compared to those by the PI-control for the three scan rates in Fig. 10, respectively, where the low-speed 2-Hz scan image was used as the reference.

The experimental results showed the efficacy of the proposed approach in improving the topography tracking in high-speed tapping mode imaging. First, by using the pro-

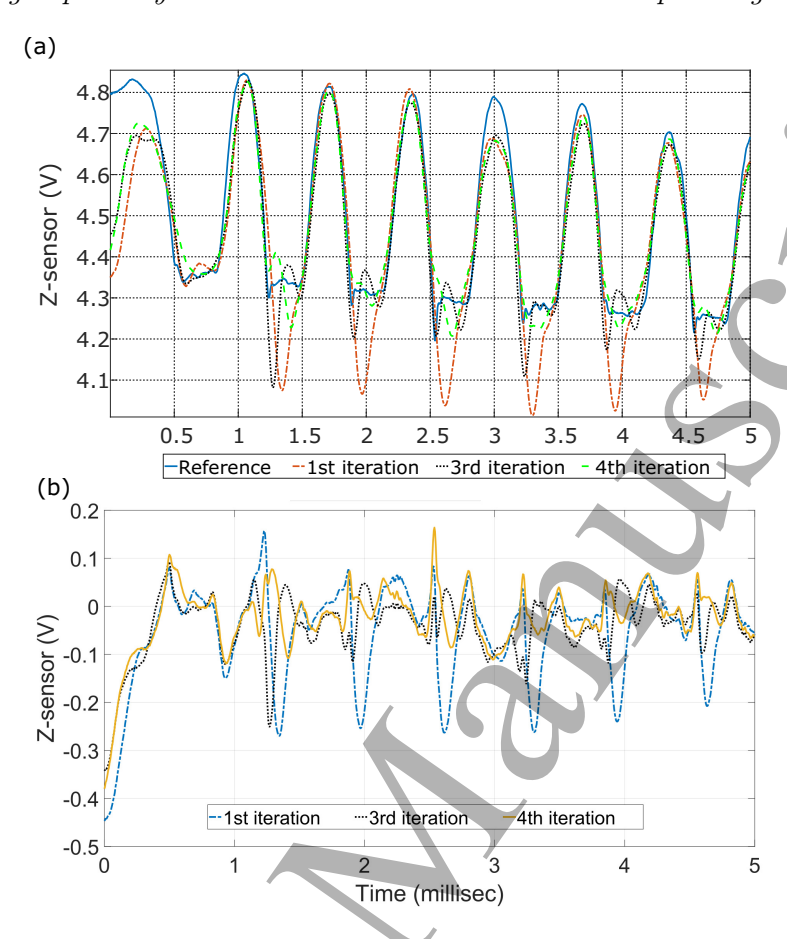
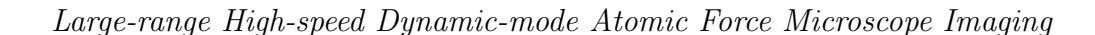


Figure 4. Comparison of (a) the z-axis piezoelectric actuator displacements obtained by using the AT-MLM in four repetitive scannings on the first line at the scan rate of 100 Hz to that obtained by the PI control at the scan rate of 2 Hz scan rate, and (b) displacement error of each scanning with respect to that obtained with PI control at 2 Hz as the reference, respectively.

posed experimental-based on-site free-scanning method (see Subsec. II.3), the lateral-coupling-caused deflection deviation was effectively removed. As shown in Fig. 3, the lateral-coupling-caused TM-deflection fluctuation was pronounced—the envelop change of the TM-deflection in Fig. 3 (a) caused by the lateral coupling effect was as large as 2 V, 10 times larger of that due to the topography variation of the calibration sample. By using the proposed method, this lateral coupling effect was completely removed—the fluctuation of the TM-deflection was now around the noise level with a small mean value around 20 mV. Secondly, online convergence was achieved by using the proposed TD-IIC algorithm in the AT-MLM control. As shown in Fig. 4, tracking of the sample topography on the first scanline converged in only 3-4 iterations, with the relative tracking error reduced by 84.7%. These three improvements in lateral-coupling removal, rapid convergence and accurate topography tracking in the repetitive scanning on the first line, and the adaptive TM-amplitude set-point adjustment directly contributed to the performance of the proposed AT-MLM technique.



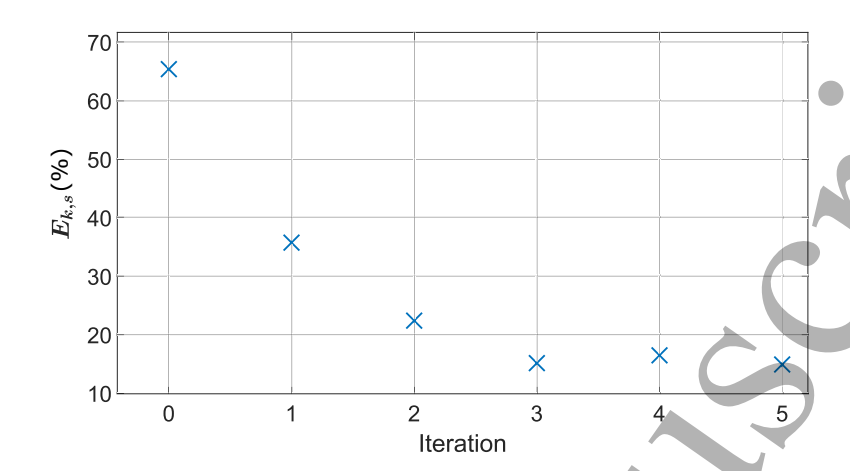


Figure 5. The relative 2-norm error of the z-axis displacement obtained in each iteration, $\mathbf{E}_{k,2}(\%)$, during the repetitive scanning on the first line for the scan rate of 100 Hz.

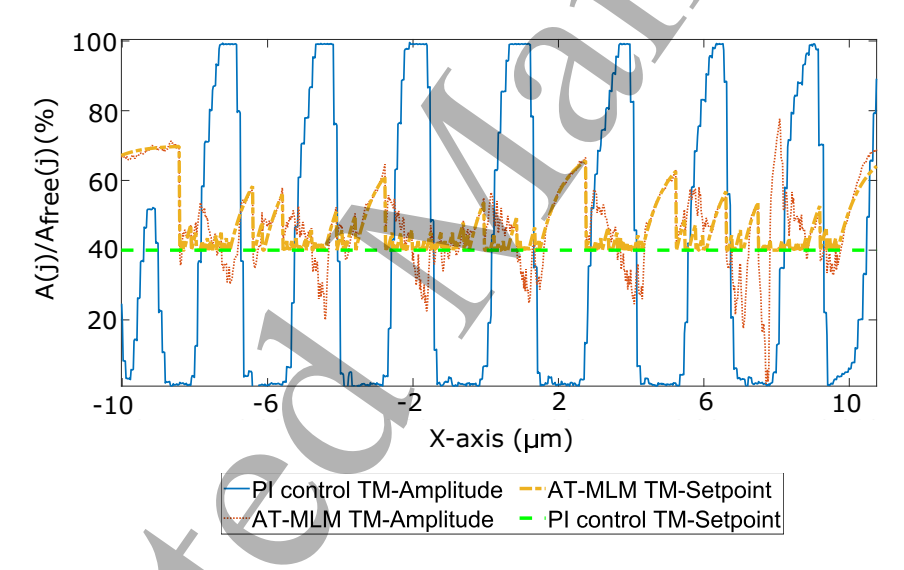


Figure 6. The tapping amplitude ratio of AT-MLM algorithm and PI control, with comparison to the AT-MLM adjusted setpoint and pre-chosen PI control setpoint of a random chosen cross-section (aqua-colored line in Fig. 7) for the scan rate of 100 Hz.

The imaging results obtained in the experiment demonstrated that the speed of tapping-mode, large range AFM imaging can be significantly increased by using the proposed approach. It can be seen that the image quality of the topography obtained by using the AT-MLM technique at 100 Hz compared well to that obtained by tapping mode imaging at 2 Hz (compare Fig. 7(a) to Fig. 7(d)). Both images presented sharp edges of the square-shaped pitches in Fig. 8, whereas these topography characteristics of the sample was severely distorted in the conventional tapping mode imaging result at 100 Hz scan rate. The overall imaging error was reduced from 73% to 14% (see Fig. 10 (a)). Moreover, the experimental results also showed the efficacy of the proposed adaptive set-point adjustment in imaging quality improvement—resulting in sharper edges of the pitches

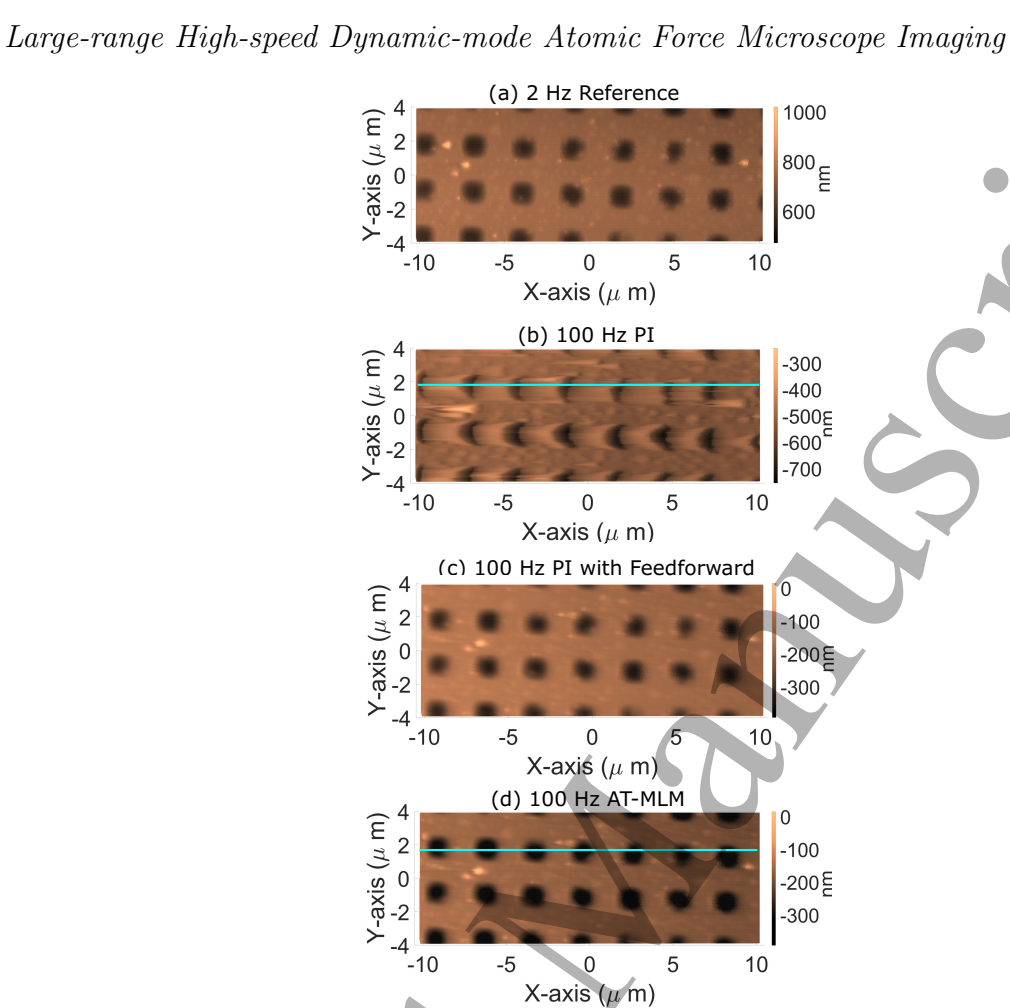


Figure 7. Comparison of the topography image of the calibration sample obtained by using the PI-feedback alone at the scan rate of (a) 2 Hz and (b) 100 Hz, (c) the PI-feedback + TDIIC feedforward control and (d) the proposed AT-MLM technique at the scan rate of 100 Hz, respectively.

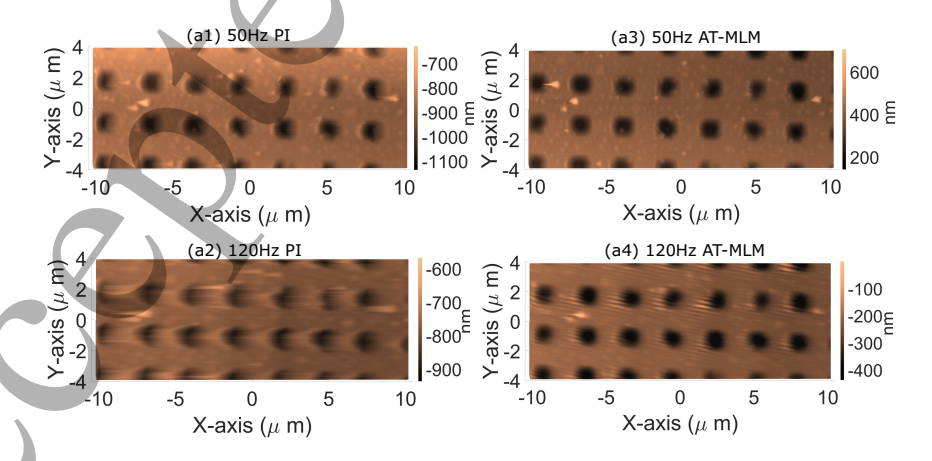


Figure 8. Comparison of the topography image of the calibration sample obtained by using the AT-MLM technique at the scan rate of (a3) 50 Hz, (a4) 120 Hz, to those by using the PI-feedback alone at the scan rate of (a1) 50 Hz, (a2) 120 Hz, respectively.

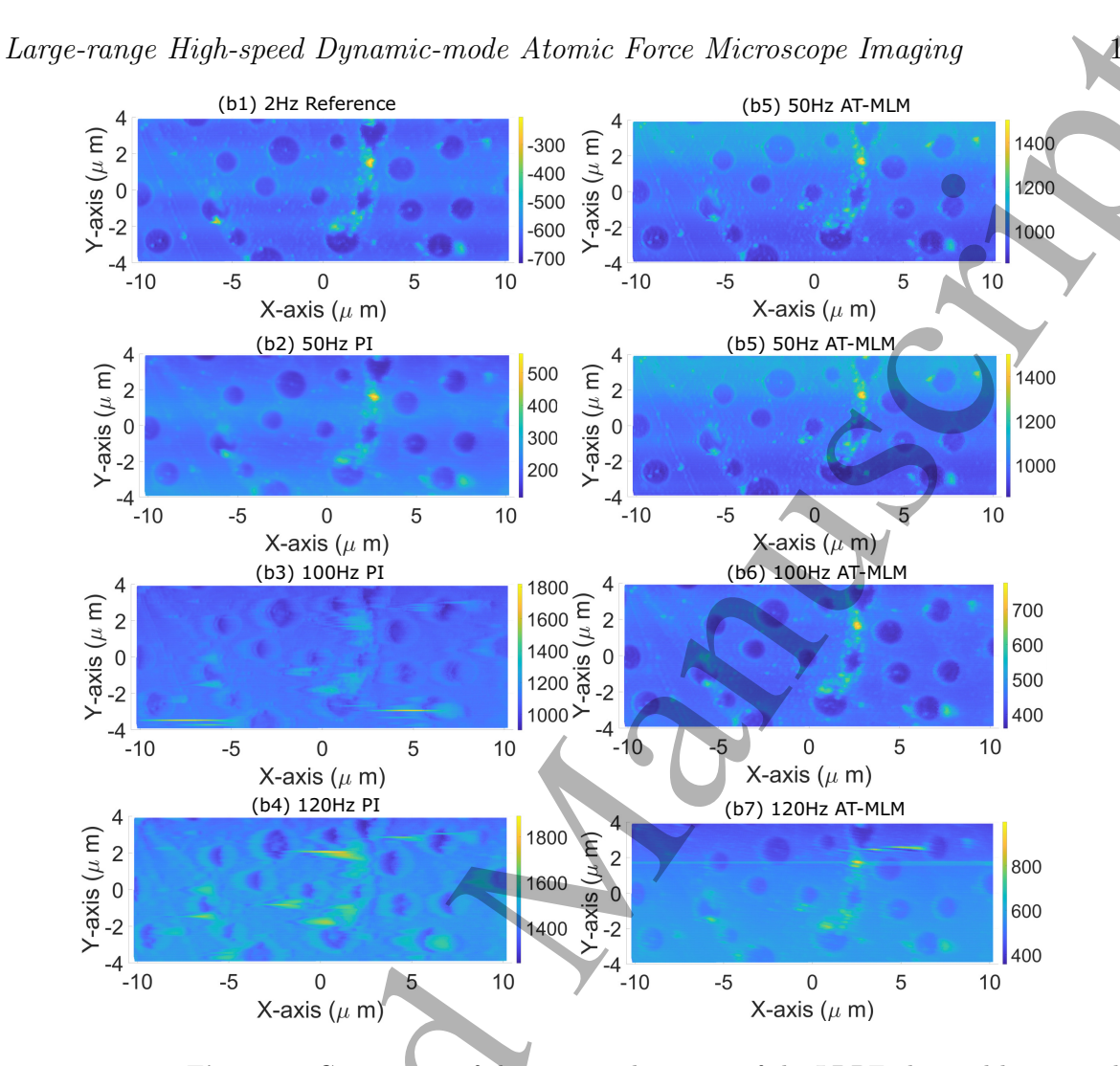


Figure 9. Comparison of the topography image of the LDPE obtained by using the AT-MLM technique at the scan rate of (b5) 50 Hz, (b6) 100 Hz, and (b7) 120 Hz, to those by using the PI-feedback alone at the scan rate of (b2) 50 Hz, (b3) 100 Hz, and (b4) 120 Hz, respectively.

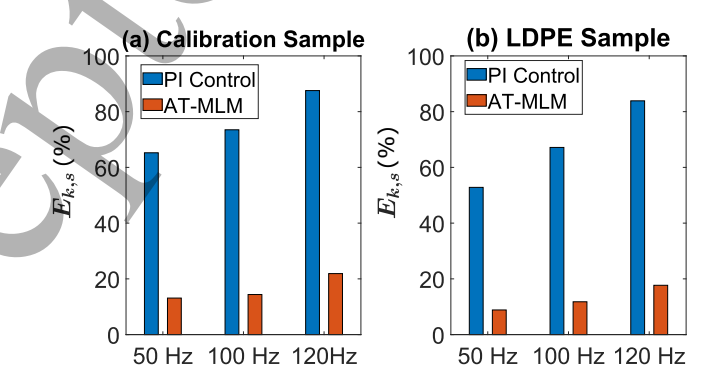


Figure 10. Comparison of the 2-norm error of (a) Calibration Sample and (b) LDPE sample, respectively.

captured in the topography image (compare Fig. 7 (c) to (d)). These improvements in high-speed, large-range imaging was consistent across all three scan rates tested in

Large-range High-speed Dynamic-mode Atomic Force Microscope Imaging

the experiment, as shown in Fig. 8. The overall imaging error was reduced from the conventional tapping mode imaging by 80% and 75% for the scan rate of 50 Hz and 120 Hz, respectively (see Fig. 10 (a)). This significant increase of imaging speed while maintaining the imaging quality can also been clearly seen in the imaging results for the LDPE sample (see Fig. 9).

Two features of the proposed AT-MLM technique were illustrated through the experimental results. At the scan size of 20 μ m, the probe scanning speed on the sample surface reached 4 mm/sec. and 4.8 mm/sec. for the scan rate of 100 Hz and 120 Hz. Such a high-speed probe scanning has not been reported in the literature (with the imaging quality maintained). As a comparison, the probe scanning speed in the high-speed tapping mode imaging reported in [15] was at 0.48 mm/sec for the scan size of 150 nm, 10 times slower than that achieved in this work. Another feature is that the proposed AT-MLM was capable of imaging samples of high aspect ratio. With vertical edges and sample height at 180 nm, the calibration sample was challenging to image at high speed, whereas in the high-speed tapping mode imaging in [15], the sample height was below 18 nm, 10 times smaller than that imaged in this work, and the sample topography was smooth. Therefore, the experimental results demonstrated the efficacy of the proposed approach in achieving high-speed large-range tapping-mode imaging on AFM.

5. Conclusion

A hardware-software integrated approach is proposed for high-speed, large-range tapping-mode imaging on AFM. The recently developed AMLM technique was further enhanced and integrated with a FPGA high-speed data processing platform on an AFM system with nanopositioning system of increased bandwidth. Moreover, an adaptive tapping multi-loop mode (AT-MLM) was proposed to adaptively minimize the tapping force while maintaining the imaging quality under high speed scanning. The efficacy of the proposed E-AMLM imaging was demonstrated by imaging a calibration sample and a LDPE sample at different scanning speeds (50 to 120 Hz) in experiment. The experiment results showed that by using the proposed technique, the imaging speed was significantly increased.

Acknowledgment

This work was supported by the NSF grants CMMI-1851907, CMMI-1663055, and IDBR 1952823.

Reference

[1] N. Gadegaard (2006) "Atomic force microscopy in biology: technology and techniques", Biotechnic & Histochemistry, 81:2-3, 87-97, DOI: 10.1080/10520290600783143

- [2] J. Ren, Q. Zou, B. Li, and Z. Lin, "High-speed atomic force microscope imaging: Adaptive multiloop mode," Phys. Rev. E, vol. 90, pp. 012405, July 2014.
- [3] J. Ren and Q. Zou, "High-speed adaptive contact-mode atomic force microscopy imaging with near-minimum-force", Review of Scientific Instruments 85, 073706 (2014)
- [4] C. Su, L. Huang, K. Kjoller, Direct measurement of tapping force with a cantilever deflection force sensor, Ultramicroscopy, Volume 100, Issues 3–4, 2004, Pages 233-239, ISSN 0304-3991, https://doi.org/10.1016/j.ultramic.2003.11.007.
- [5] T. Ando, "High-speed AFM imaging", Current Opinion in Structural Biology, vol. 28, pp. 63-68, October 2014.
- [6] Y. K. Yong, S. O. R. Moheimani, "Collocated Z-Axis Control of a High-Speed Nanopositioner for Video-Rate Atomic Force Microscopy", IEEE Transactions on Nanotechnology, vol. 14, pp. 338-345, March 2015.
- [7] L. M. Picco, L. Bozec, A. Ulcinas, D. J. Engledew, M. Antognozzi, M. A. Horton and M. J. Miles, "Breaking the speed limit with atomic force microscopy", Nanotechnology, vol. 18, pp. 044030, 2007.
- [8] C. Su, L. Huang, and K. Kjoller, "Direct measurement of tapping force with a cantilever deflection force sensor", Ultramicroscopy, vol. 100, pp. 233-239, 2004.
- [9] T. Sulchek, G. G. Yaralioglu, and C. F. Quate, "Characterization and optimization of scan speed for tapping-mode atomic force microscopy", Review of Scientific Instruments, vol. 73, pp. 2928, 2002.
- [10] A. Keyvani, H. Sadeghian, M. S. Tamer, J. F. L. Goosen, and F. V. Keulen, "Minimizing tip-sample forces and enhancing sensitivity in atomic force microscopy with dynamically compliant cantilevers", Journal of Applied Physics, vol. 121, pp. 244505, 2017.
- [11] Dikecoglu, F. Begum, et al. "Force and time-dependent self-assembly, disruption and recovery of supramolecular peptide amphiphile nanofibers." Nanotechnology 29.28 (2018): 285701.
- [12] W. Li, et al. "Simultaneous nanoscale imaging of chemical and architectural heterogeneity on yeast cell wall particles." Langmuir 36.22 (2020): 6169-6177.
- [13] Gusenbauer, Claudia, et al. "Nanoscale chemical features of the natural fibrous material wood." Biomacromolecules 21.10 (2020): 4244-4252.
- [14] B. Rogers, T. Sulchek, K. Murray, D. York, M. Jones, L. Manning, S. Malekos, B. Beneschott, and J. D. Adams, "High speed tapping mode atomic force microscopy in liquid using an insulated piezoelectric cantilever", Review of Scientific Instruments, vol. 74, pp. 4683, 2003.
- [15] T. Ando, T. Uchihashi and N. Kodera, "High-Speed AFM and Applications to Biomolecular Systems", Annual Review of Biophysics, vol. 42, pp. 393-414, May 2013.
- [16] D. R. Sahoo, A. Sebastian, and M. V. Salapaka, "Transient-signal-based sample-detection in atomic force microscopy", Appl. Phys. Lett., vol. 83, pp. 5521, 2003.
- [17] K. S. Karvinen and S. O. R. Moheimani, "A high-bandwidth amplitude estimation technique for dynamic mode atomic force microscopy", Review of Scientific Instruments 85, 023707 (2014) https://doi.org/10.1063/1.4865841
- [18] J. Chen, and Q. Zou. "High-speed large-range dynamic-mode atomic force microscope imaging: Adaptive tapping approach via Field Programmable Gate Array." 2020 American Control Conference (ACC). IEEE, 2020.
- [19] M. S. Rana, H. R. Pota, and I. R. Petersen, "High-Speed AFM Image Scanning Using Observer-Based MPC-Notch Control", IEEE Transactions on Nanotechnology, vol. 12, pp. 246 254, March 2013.
- [20] G. Clayton, et al. "A review of feedforward control approaches in nanopositioning for high-speed SPM." (2009): 061101.
- [21] G. Schitter, et al. "Design and modeling of a high-speed AFM-scanner." IEEE Transactions on Control Systems Technology 15.5 (2007): 906-915.
- [22] S. Salapaka, A. Sebastian, et al. "High bandwidth nano-positioner: A robust control approach", Review of Scientific Instruments 73, 3232-3241 (2002) https://doi.org/10.1063/1.1499533

Large-range High-speed Dynamic-mode Atomic Force Microscope Imaging

[23] Y. Wu, Y. Fang, C. Wang, C. Liu and Z. Fan "A high-speed atomic force microscopy with super resolution based on path planning scanning", Ultramicroscopy, Vol. 213, pp. 112991, 2020

- [24] J. Ren, Q. Zou, "High-speed dynamic-mode atomic force microscopy imaging of polymers: an adaptive multiloop-mode approach", Beilstein J. Nanotechnol., vol. 8, pp. 1563-1570, Aug. 2017.
- [25] M. G. Ruppert and S. O. R. Moheimani, "Multimode Q control in Tapping-Mode AFM: Enabling Imaging on Higher Flexural Eigenmodes", IEEE Transactions on Control Systems Technology, vol. 24, pp. 1149-1159, Oct. 2015.
- [26] Q.Zhong, D.Inniss, K.Kjoller, and V.B.Elings, "Fractured polymer/silica fiber surface studied by tapping mode atomic force microscopy", Surface Science Letters, vol. 290, pp. L688-L692, June 1993.
- [27] K. S. Kim, Q. Zou, "A Modeling-Free Inversion-Based Iterative Feedforward Control for Precision Output Tracking of Linear Time-Invariant Systems", IEEE/ASME Transactions on Mechatronics, vol. 18, ppl. 1767 - 1777, Sep. 2012.